Confinement and Proton Transfer in NAFION Thin Films

ARTICLE *in* MACROMOLECULES · JANUARY 2013

Impact Factor: 5.8 · DOI: 10.1021/ma3011137

2 AUTHORS, INCLUDING:

Shudipto Konika Dishari
Pennsylvania State University
9 PUBLICATIONS **113** CITATIONS

SEE PROFILE

Macromolecules

Article

pubs.acs.org/Macromolecules

Confinement and Proton Transfer in NAFION Thin Films

Shudipto K. Dishari and Michael A. Hickner*

Department of Materials Science and Engineering, The Pennsylvania State University, University Park, Pennsylvania 16802, United States

Supporting Information

ABSTRACT: Steady-state fluorescence measurements of two different probe molecules were undertaken to explore the water solvation environment and molecular mobility in 70–600 nm NAFION thin films and 50 μm thick NAFION membranes. The influence of film thickness, hydration number, and polymer–substrate interaction on proton dissociation and transfer from photoexcited 8-hydroxypyrene-1,3,6-trisulfonic acid sodium salt (HPTS) to the surrounding solvation environment and the local mobility of 9-(2-carboxy-2-cyanovinyl)julolidine (CCVJ) in the samples were investigated. Deprotonation of the photoacidic HPTS was suppressed in thinner films in both H^+ and Na^+ counterion-form samples. This observation revealed the presence of a solvation environment that was suitable for accepting and transporting protons in thinner films compared to a better proton accepting environment in thick films in which higher deprotonation of HPTS was observed. The results from HPTS studies indicated that smaller ionic domains formed in thinner samples regardless of the substrate type. NAFION membrane exhibited a continuous hydration induced plasticization as monitored by a steady decrease in CCVJ fluorescence intensity which was a result of a more mobile local environment in the 50 μm thick membrane. The plasticization behavior of the membrane was in contrast to restricted mobility and antiplasticization observed in thin films. The thickness-normalized fluorescence intensity of CCVJ in the thin film samples implied lower polymer chain mobility in the dry state in thin films on native oxide silicon (n-SiO_2) substrates compared to thin films on Au substrates. At similar hydration number, higher CCVJ fluorescence values were observed for hydrated films on n-SiO_2 compared to samples on Au, which was attributed to strong polymer-SiO_2 interactions at the interface.

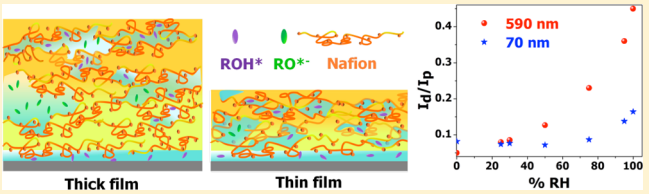

INTRODUCTION

Thin polymer films have distinct physical properties compared to bulk samples due to interfacial confinement at the polymer–substrate boundary, free surface effects, and specific interactions between the polymer chains and the surface. The effect of confinement has been observed in the glass transition temperature (T_g),[1] rheology,[2] swelling kinetics,[3] and water uptake/proton diffusion behavior[4] of thin films for many different types of polymers. In order to understand thin film confinement effects on proton transfer[5−8] and mechanical properties,[9] hydrogels,[5,9] reverse micelles,[10] and thin polymer films[4,6−8] are often employed where water molecules were confined within nanoscale cavities and experienced extremely viscous environments.[11]

In addition to T_g[11] measurements and probing thin films using neutron reflectivity[12,13]and X-ray reflectivity,[14] reduced polymer mobility at polymer/solid interfaces in thin polymer films (~40–1000 nm) has been measured using sensitive fluorescence-based techniques, like fluorescence recovery after photobleaching (FRAP)[15] and steady state fluorescence measurements.[16−18] Miller et al. reported mobility-sensitive julolidine based fluorescent rotor probes to monitor water uptake in thick PMMA films.[17] The fluorescence intensity of rotor probes changes in response to local mobility of water and polymer chains due to intramolecular rotational/torsional motion.[17,19] Both the fluorescence intensity and the quantum yield of CCVJ increase with an increase in viscosity of the local environment. Under confinement where both polymer and water motion is suppressed the higher viscosity increase the fluorescence signal from the rotor probe. Employing this type of dye in thin films and measuring its steady state fluorescence is a straightforward way to estimate the relative mobility of the water/polymer mixture under various conditions. In an earlier report, we demonstrated that film thickness and hydration have significant influence on the mobility of thin NAFION films on n-SiO_2 using the rotor probe CCVJ (Figure 1, left).[20]

A few studies have shown that thin films of NAFION exhibit anomalous conductivity behavior compared to bulk films, but the mechanisms for these conductivity results have not been

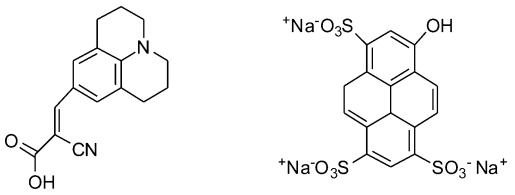

Figure 1. Chemical structure of CCVJ (left) and HPTS (right).

Received: May 31, 2012
Revised: November 16, 2012
Published: January 9, 2013

probed in detail.[4] NAFION has shown very high proton conduction[21] upon hydration in its membrane form. Its hydrophobic fluorocarbon-based backbone provides the membrane unique chemical, mechanical, and thermal stability, while the hydrophilic sulfonic acid groups are important for water sorption and proton donation to the water phase. Information about the nature of proton transport and proton mobility in NAFION nanoscopic channels is crucial in fuel cell operation and the proton transport mechanisms operating in membranes have been approached using a variety of experimental and modeling techniques.[22,23] In fuel cell devices, a thin NAFION ionomer layer (~2−30 nm thick) coats the platinum/carbon catalyst particles to promote proton conduction between membrane and the electrochemically active catalytic sites.[24] Thus, measurements of the physical properties and proton transport rates of thin NAFION films are needed to understand the properties of the thin polymer layer at the catalytic interface. Additionally, since the proton transport and physical properties are intimately tied to the water behavior in the material, measurements of water's interactions in these thin films are important.

Proton diffusion is a function of water content and the hydrophilic−hydrophobic domains' geometry[25] and the mobility of water in NAFION films govern the diffusion of protons within the material.[22,26,27] Excited state proton transfer (ESPT) probes are widely used in fluorescence-based investigations of confinement effects on proton transport.[28−32] The pK_a values of these hydroxyaromatic photoacids, like HPTS (Figure 1, right), drop dramatically when the molecules are excited by UV light. The deprotonation of HPTS can be observed in its emission spectrum when a proton from the hydroxyl group of the dye is released to the surrounding environment upon photoexcitation:

$$ROH^* \leftrightarrows RO^{*-} + H^+ \quad (1)$$

Here ROH* and RO*$^-$ correspond to the protonated and deprotonated states of HPTS, respectively. The populations of protonated and deprotonated states of the dye depend on the proton-accepting nature of the surrounding environment. In a hydrated film, more deprotonation of the dye suggests that the water molecules are highly mobile and thus good proton acceptors. If the water is less mobile, it is not as good of a proton acceptor and there will be a larger fraction of protonated dye states compared to deprotonated states. Monitoring the extent of deprotonation of HPTS enables the probing of proton transfer characteristics of water domains inside films and membranes. Fayer et al.[30−32] employed HPTS to probe proton diffusion and proton concentration in nancoscopic domains of unannealed N117 NAFION membrane (~183 μm thick) and sodium bis(2-ethylhexyl) sulfosuccinate (Aerosol OT or AOT) reverse micelles. The proton transfer rate was suppressed with a decrease in size of the reverse micelles[10] where a sharp decline in ESPT was observed for a reverse micelle of diameter ≤4 nm. The proton dissociation rate was 100 times lower in reverse micelles of size ~1.7 nm compared to bulk water.

Interfacial bonding of a polymer to a solid interface reduces the conformational entropy of the chain. The segmental mobility of PMMA[33] was restricted in thin films due to strong hydrogen bonding interactions with n-SiO_2 substrate, but changing the substrate to Au weakened the interaction and enhanced polymer mobility. The confining interface can also impede the orientational relaxation of water (hydrogen bond structural randomization), a prerequisite for efficient proton conduction.[34] The morphological structure of thin NAFION films (containing both water and polymer) depends on the interaction of polymer chains with the substrate. Different NAFION morphologies were observed on n-SiO_2 and octadecyl silane treated Si-wafer due to different interactions of the hydrophilic and hydrophobic substrates with the acidic polymer.[35] Dura, et al. showed the presence of lamellar ordering in the plane of the substrate for thin NAFION films on n-SiO_2 where no such layers were present on an Au surface.[13] Also for NAFION films on Pt and carbon surfaces, long-range structural arrangement and the interfacial structure of the polymer was reported to be dependent on the nature of substrate.[36] Paul, et al. proposed that the ordering of NAFION changes as a function of thickness on n-SiO_2 for films that were adsorbed on the substrate from solution, which is a different preparation method than most spun-cast samples investigated in the literature.[4] These authors found an abrupt drop in proton conductivity when the NAFION film thickness decreased from ~310 to 60 nm. Kongkanand focused on water uptake in drop cast thin NAFION films on Au.[37] Similar hydration numbers for films from 3000 to 500 nm were observed, but the water uptake systematically declined as the film thicknesses were reduced to 33 nm. These results suggested that the lower proton conductivity in thinner NAFION films[38] might originate from events other than water uptake and the origins of the decrease in water uptake are yet to be probed in detail. The community has learned from membrane studies that the polymer morphology, water uptake, water mobility, and proton transport are interconnected. The emerging studies on thin films suggest that these properties are altered compared to the membrane state and highlight the importance of comprehensive studies of thin film ordering, hydration, and dynamics.

In this work, the proton solvation and local mobility of NAFION thin films and membranes were compared to determine how thickness influences these fundamental parameters that ultimately determine proton transport. Proton solvation in acid (H^+-form) and sodium neutralized (Na^+-form) NAFION thin films and membranes were compared through steady-state fluorescence measurements of HPTS incorporated into the films. In the H^+-from, the proton originating from the sulfonic acid groups of the polymer may retard the deprotonation of HPTS. Thus, the purpose of studying fluorescence of HPTS in Na^+−NAFION was to avoid interference of the local proton concentration from the sulfonic acid groups on dye deprotonation.[32] The thickness and interfacial effects on mobility in thin NAFION films were explored on Au and n-SiO_2 substrates using CCVJ steady-state fluorescence measurements and compared to measurements on thick membranes. The connection between proton solvation and mobility was revealed for thin films. The current study presents an explanation for why proton transport is hindered in thin film architectures.

EXPERIMENTAL METHODS

Materials. 9-(2-Carboxy-2-cyanovinyl)julolidine, CCVJ and 8-hydroxypyrene-1,3,6-trisulfonic acid sodium salt (HPTS) were purchased from Sigma-Aldrich (St. Louis, MO). A 20 wt % NAFION solution (DE2020, EW ~ 1000) and NR212 membrane (EW ~ 1100, thickness = 50 μm)[39] were purchased from Ion Power, Inc. (New Castle, DE).

Film and Membrane Preparation. First, a 20 wt % H^+−NAFION solution was diluted with ethanol to achieve the desired polymer concentrations for spin coating. CCVJ in DMSO (5 mg mL^{-1}) was added to 10 wt %, 5 and 2 wt % NAFION solutions to

dx.doi.org/10.1021/ma3011137 | Macromolecules 2013, 46, 413−421

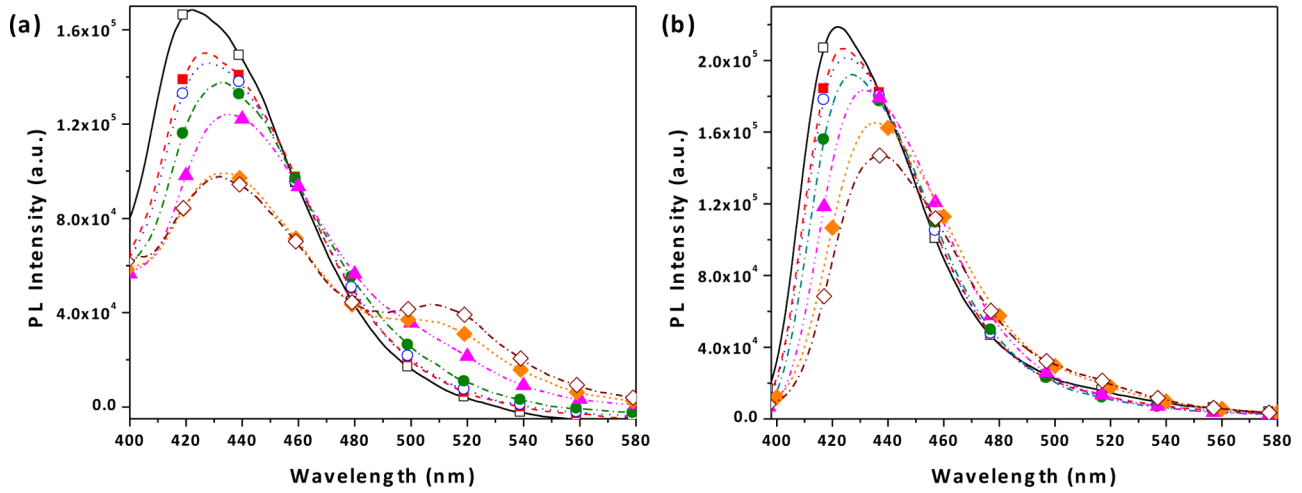

Figure 2. Fluorescence response of (a) 590 nm and (b) 70 nm H^+−NAFION films containing HPTS (λ_{exc} 370 nm, λ_{em} 390−590 nm) on n-SiO_2 ((black □) 0%, (red ■) 25%, (blue ○) 30%, (green ●) 50%, (pink ▲) 75%, (orange ◆) 95%, (brown ◇) 100% RH).

yield a dye concentration of 0.018 wt % (0.6 mM, unless otherwise stated). For a separate set of samples containing HPTS, the concentration of HPTS was maintained at 0.25 mM in all NAFION solutions used to prepare thin films. Si wafers (single-side polished low conductivity, Silicon Quest International, Inc., Santa Clara, CA) were coated with a 5 nm thick Cr layer and a 50 nm thick Au layer via e-beam evaporation to yield Au substrates. Bare silicon with native oxide (n-SiO_2) and Au-wafers were cut into (2 cm × 2.5 cm) pieces, rinsed with methanol, dried under flowing air, and UV−ozone treated for 20 min under flowing nitrogen. The spin coating speed was maintained at 3000 rpm. The wt % of NAFION in solution was varied to yield films of the desired thickness from 70 to 600 nm. All films and membranes were dried at 42 °C for 3 h, annealed at 100 °C for 7 h, and cooled to room temperature for 12 h while maintaining vacuum for all steps. The films were then characterized by exposing to air with controlled humidity. This type of annealing under dry conditions lowers the hydration number at a specific relative humidity for NAFION films compared to those treated in liquid water before characterization.[26]

Na^+-form NAFION was prepared by titrating 20 wt % NAFION solution (H^+-form) with a 15 wt % excess of aqueous NaOH solution under vigorous stirring for 24 h. The neutralized NAFION solution was further diluted with ethanol to achieve the desired concentration of Na^+−NAFION in solution.

NR212 membranes were annealed under the same conditions as the thin films, soaked in dye solution ([HPTS] = 0.1 M; [CCVJ] = 0.018 wt % in 1: 1 C_2H_5OH: water solution) for 18 h, rinsed, and dried for 1 d in vacuum oven at 42 °C. Annealed membranes were Na^+-exchanged by soaking in NaCl (1 M) solution for 1 d and then rinsed with water prior to annealing and immersion in dye solution.

Water Uptake. Water uptake was measured using a quartz crystal microbalance (QCM) (Maxtek/Inficon, East Syracuse, NY) and Saurbrey analysis. n-SiO_2 and Au-coated 6 MHz crystals (Tangidyne, Greenville, SC) were employed as QCM substrates. A custom-built plastic vessel was employed as the QCM humidity chamber. The hydration number (λ) was calculated as the number of moles of water per mole of sulfonate groups in the polymer and the error bars were calculated from the standard deviations of experiments performed in triplicate on separately prepared samples.

Thickness. The thickness of all polymer films was measured using variable angle spectroscopic ellipsometry (V.A.S.E., J. A. Woollam Co., Inc., Lincoln, NE) with a spectral range of 193−2500 nm at ambient conditions. Bare silicon with its native oxice and Au-coated silicon wafers were used as references and the polymer film was modeled as a homogeneous material with uniform optical constants. The thickness values were compared with those calculated from polymer mass in the QCM experiments assuming NAFION density of 2.0 g cm^{-3}.

Fluorescence. Steady state fluorescence of thin films on substrates and membranes was measured using a Photon Technology International, Inc. (Birmingham, NJ) QuantaMaster steady-state fluorimeter with 90° excitation/emission geometry and 2 nm excitation/emission bandpass slits. The excitation wavelength (λ_{exc}) for HPTS was 370 nm and emission (λ_{em}) was collected in the range from 390 to 590 nm. While λ_{exc} and λ_{em} values for CCVJ were 400 nm and 420−590 nm, respectively. The integration time was optimized for and held constant for all samples. RH-dependent fluorescence measurements were performed by connecting a custom-built RH control system to fluorimeter to produce a sample environment with specific water activity. All fluorescence measurements were conducted at 23 °C.

Humidification. Air at dewpoint was produced by a sparging system. The dewpoint humidified wet air was mixed with a stream of dry air and the flow rates of the wet and dry streams were varied to achieve a specific relative humidity. A RH probe (Omega HX15-W, Omega Engineering, Inc., Stamford, CT) was connected to the air outlet from the fluorescence or QCM humidity chamber for in situ monitoring of the relative humidity of the sample environment. It is to be noted that each sample was dried for 2 h inside the humidity chamber by purging dry air prior to increasing the RH of the test sample to remove any moisture adsorbed during sample exchange from the drying oven to the fluorimeter or QCM.

■ RESULTS AND DISCUSSION

It is to be noted that the purchased NAFION solutions and membranes contained fluorescent species[40] having an emission peak at 439 nm (370 nm excitation). Similar fluorescence was previously reported for wet[41] and dry[42] NAFION solutions. These impurities could be bleached by UV−H_2O_2 treatment in the solution state. However, the fluorescence recovered after annealing (results not shown here), so we conclude that the autofluorescence is due to the intrinsic properties of the polymer and is not from an impurity. Thus, all the fluorescence curves obtained for NAFION films with CCVJ or HPTS at a specific RH were background subtracted using films without dye at similar thickness and RH to remove the native autofluorescence of the polymer.

Figure 2 illustrates the fluorescence of HPTS for 70 and 590 nm thick H^+−NAFION films on n-SiO_2. The emission intensities at ∼421−434 nm and ∼510 nm corresponded to the protonated (I_p) and deprotonated (I_d) states of HPTS, respectively.[43]

At relative humidities of less than 50%, deprotonation of HPTS was suppressed in all the thin films, as denoted by the

dx.doi.org/10.1021/ma3011137 | Macromolecules 2013, 46, 413−421

lack of a distinct peak at 510 nm, over the range of thicknesses examined in both H^+ and Na^+-forms (see Figure S1 in Supporting Information for Na^+−NAFION samples). The reason behind the quenching of HPTS fluorescence intensity around 430 nm (I_p) without the appearance of a deprotonated state emission at 510 nm was not determined, but the possibility of a nonradiative excited state decay through association between HPTS and polymer sulfonate groups by hydrogen bonding[44] in addition to geminate recombination cannot be ruled out. The redshift observed in I_p with hydration (λ_{max} 423 nm (0% RH) to 434 nm (75% RH)) could have been due to the change in polarity of the surrounding environment of HPTS during solvation.[31,45] Because of these red shifts of the protonated peak fluorescence, the emission maximum, I_p, was found between 421 and 434 nm, while I_d was the fluorescence intensity of the deprotonated state of HPTS at 510 nm.

As the humidity was increased beyond 50% RH, a resolvable increase in emission intensity at 510 nm occurred which reflected a significant population of deprotonated HPTS. Interestingly, the thickness of the films had an influence on how much proton transfer from the dye to its surrounding environment occurred as can be seen from the calculated I_d/I_p values in Figure 3. The intensity increase of the deprotonated

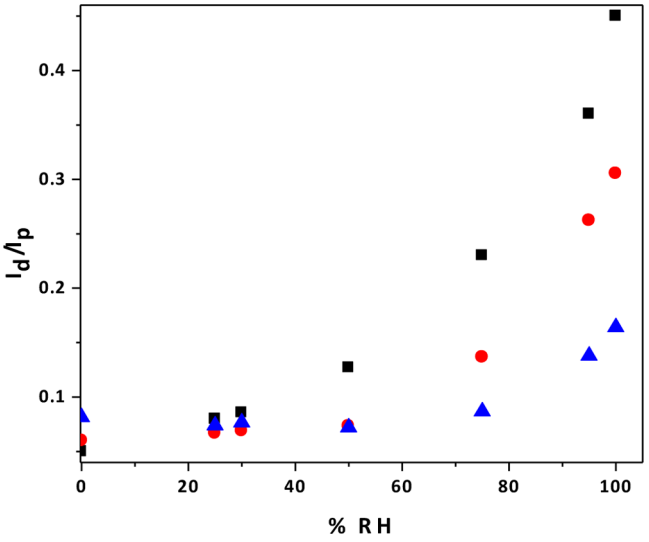

Figure 3. Ratio of fluorescence intensities of deprotonated to protonated state (I_d/I_p) of HPTS in H^+−NAFION films on n-SiO_2 surface at different relative humidity as a function of film thickness; (black ■) 590 nm; (red ●) 225 nm; (blue ▲) 70 nm.

peak with RH was low in the 70 nm thick film, Figure 2b, indicating a poor solvation environment in the thinner sample compared to the thicker sample. Na^+−NAFION films also showed a similar thickness effect but with higher I_d/I_p values (Figure S1, Supporting Information) than the corresponding H^+−NAFION samples (Figure 3) due to proton concentration effects.[32]

The hydration numbers of the thin films (Figure 4) remained low ($\lambda \sim 0$−2.2) below 50% RH except for the 70 nm H^+−NAFION films on native oxide Si wafers. The high swelling of very thin NAFION films on n-SiO_2 has been observed previously.[20] The swelling of these films is dictated by a balance of the mechanical constraint of the polymer which impedes water uptake and the solvation energy of the ionic groups which promotes water sorption. The rigid substrate

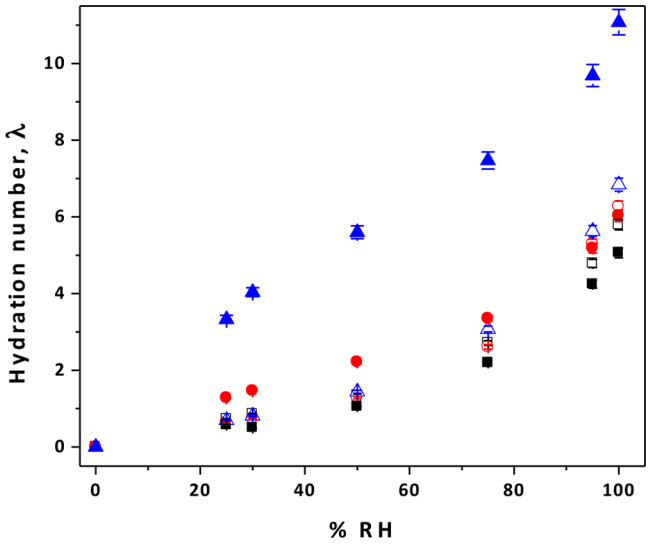

Figure 4. Hydration number as a function of water activity for spun cast H^+-form ((black ■) 615 nm (red ●) 202 nm (blue ▲) 70 nm)) and Na^+-form ((□) 610 nm; (red ○) 200 nm; (blue △) 70 nm) NAFION films on n-SiO_2 substrates.

should constrain the swelling of these films as is observed on Au surfaces. However, for the thinnest film on n-SiO_2, the swelling may be influenced by the hydrophilic nature of the substrate or a lower modulus of the 70 nm H^+-form film. Additionally, the H^+-form film may have a different morphology than the Na^+-form film as a result of the spin-casting and solvent evaporation process. At this time, we do not have enough information to isolate any of these specific factors that causes variations in the swelling of NAFION films with thickness. These mechanistic aspects of swelling in thin NAFION films will be probed in future work.

At low RH, inhibited proton transfer from excited HPTS to its environment could be attributed to the location of HPTS inside the film and the size and connectivity of the confined water domains. HPTS is a hydrophilic and negatively charged dye and tends to reside in the bulk water pools instead of being close to the sulfonate groups of NAFION in the interfacial regions due to like charge repulsion. However, with increasing hydration, water will solvate the hydrophilic sulfonate groups of the polymer at the water domain-polymer interface first. Once the solvation of the ionic groups is complete, water tends to form pools in the hydrophilic domains of the polymer. Therefore, in a film with low hydration, HPTS is likely found at the water−NAFION interface where the water is less mobile and the solvation environment is not favorable for proton transfer. Fayer estimated the proton concentration, $[H^+]$, of water domains by comparing the I_d/I_p values of HPTS in H^+−NAFION membrane with that in HCl solutions.[32] An I_d/I_p value of 0.25 (at $\lambda \sim 2.25$) corresponded to HCl concentration of 6 M. Such a high value of the local $[H^+]$ points toward HPTS remaining protonated in the excited state.

At higher levels of hydration where $\lambda > 2.2$, the thickness effect on the fluorescence behavior of HPTS was prominent and I_d/I_p increased significantly for thickner films. Fayer[32] observed the onset of deprotonation at similar λ values in H^+−NAFION membranes. It is worth noting that the declining trend of I_d/I_p with decreasing film thickness at a certain RH above 75% was not accompanied by a decrease in λ with thickness. This result demonstrates that at high RH, the

dx.doi.org/10.1021/ma3011137 | Macromolecules 2013, 46, 413−421

solvation environment is significantly influenced by water confinement and hydrophilic domain size changes induced by polymer thickness and not by the extent of hydration. At 100% RH, the λ values of the above-mentioned films (except ~70 nm thick H^+–NAFION film) reached a maximum of ~6.8. It was reported that 4–6 water molecules are required for solvation of the sulfonate headgroup of an AOT reverse micelle.[10,46] The hydration numbers measured in these thin films indicate that the majority of the water sorbed in the samples was involved in solvating the ionic groups and there was little uptake of bulk-like water. This water confinement severely affected the deprotonation of HPTS in ultrathin films. In spite of higher values of λ for the 70 nm H^+–NAFION film (~11 at 100% RH) (Figure 4), the weakest deprotonation of the series (Figures 2b and 3) was observed over the entire RH range for this thinnest sample. We believe that fundamental changes in the behavior of the thin polymer film, namely the domain structure, influenced its hydration environment and prevented deprotonation of the photoacid.

It has been previously established that thin NAFION films likely have different hydrophilic/hydrophobic domain morphologies than bulk membranes.[4,13,35] To support these structural observations and our measurements on deprotonation further, the size (Stokes radii) of the water pools can be roughly approximated by comparing the hydration number of NAFION films with the hydration number of AOT reverse micelles. The size of water pools when the water molecules are completely randomized ($\lambda \sim 22$) was reported to be 7.5 nm.[32,47] While at $\lambda \sim 2$, HPTS experienced a water environment having similar characteristics to a 2 nm water pool in AOT. The largest dimension of HPTS is approximately 1 nm. In such a confined environment at low hydration number, both HPTS and water would be relatively immobile. Rotational mobility of water plays a pivotal role in proton diffusion. In bulk water, ESPT of HPTS occurs very quickly (~80 ps in H^+–NAFION membrane),[32] while it is much slower at low hydration numbers (~930 ps at $\lambda \sim 1$).[32] For facile proton transfer to occur, freedom for reorientational relaxation and hydrogen bond randomization of water molecules are required. Protons can diffuse quickly when ultrafast proton transfer and hydrogen bond rearrangement occurs through extended water chains. IR pump–probe anisotropy of water in a NAFION membrane revealed that the presence of adjacent water molecules for donation/acceptation of hydrogen bonds is less likely at low hydration (λ~1).[30] These observations strengthen the arguement that the interconnection between hydrophilic phases in NAFION may be impeded in thin films as schematically shown in Scheme 1.

Reduced confinement effects and a better solvation environment were observed in free-standing membranes where significantly higher I_d/I_p values were observed compared to thin films (Figure 5, parts a and b). Na^+-form NR212 membrane showed a 2-fold higher deprotonation of HPTS versus the H^+-form membrane even at lower hydration numbers due to local proton concentration effects.[32,48] At 100% RH, the hydration number for a 70 nm thick H^+–NAFION film ($\lambda \sim 11$, Figure 4) was greater than that of the H^+-membrane ($\lambda \sim 9.2$, Figure S2, Supporting Information). The large water uptake of thin NAFION films on n-SiO_2 has been observed previously[20] and may be due to the lamellar morphologies in these thin-film samples.[13] However, at equivalent hydration number, the deprotonation of the HPTS dye was 10× lower in the 70 nm film compared to the membrane which indicated strong confinement of the solvation environment in the thin film.

Scheme 1. Representation of Water Domain Connectivity and Proton Transfer of HPTS in Thick (590 nm) and Thin (70 nm) NAFION Films[a]

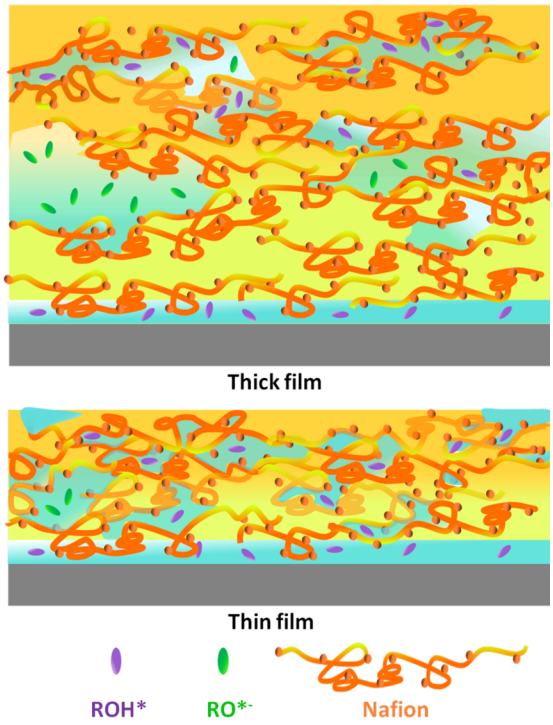

[a]ROH* and RO*$^-$ represent the protonated and deprotonated state of HPTS, respectively.

The I_d/I_p of HPTS in NAFION thin films on n-SiO_2 and Au surfaces were also compared (Figure 6). For 88 nm (Au) and 70 nm (n-SiO_2) films, the similar values of I_d/I_p indicate that the films on each surface had similar water domain sizes. Since the specific interactions of NAFION with n-SiO_2[13,49] and Au[50] are likely different as discussed in detail below, this result shows that the presence of the confined and free surfaces have an influence on the ionic domain size, no matter what the character of the confining surface is.

The HPTS data demonstrate that the phase separation characteristics, or the size of the hydrophilic domains, are different in bulk membranes compared to thin films. Reducing the thickness of block copolymer films is known to influence the phase separation of the material as the thickness of the film approaches a characteristic length scale.[51] Ionic domains in bulk NAFION membranes are very small, on the order of 5–10 nm. However, the substrate interactions that Nafion experiences can be extremely large due to the dipole, hydrogen-bonding and coulombic interactions of the sulfonate groups with the surface,[49] so there could be significant changes in the morphology of the film at thicknesses that are many multiples of the characteristic morphological length scale. From the data in Figure 5, there is clearly a thickness effect on the size of the water pools experienced by HPTS. As the sample becomes thinner, the ionic domains become smaller and less connected, which will influence the conductivity of the thin films as discussed earlier. It appears that similar trends in domain size are observed on both n-SiO_2 and Au surfaces, as detailed in Figure 6. Thus, the domain size decrease does not rely on

dx.doi.org/10.1021/ma3011137 | Macromolecules 2013, 46, 413–421

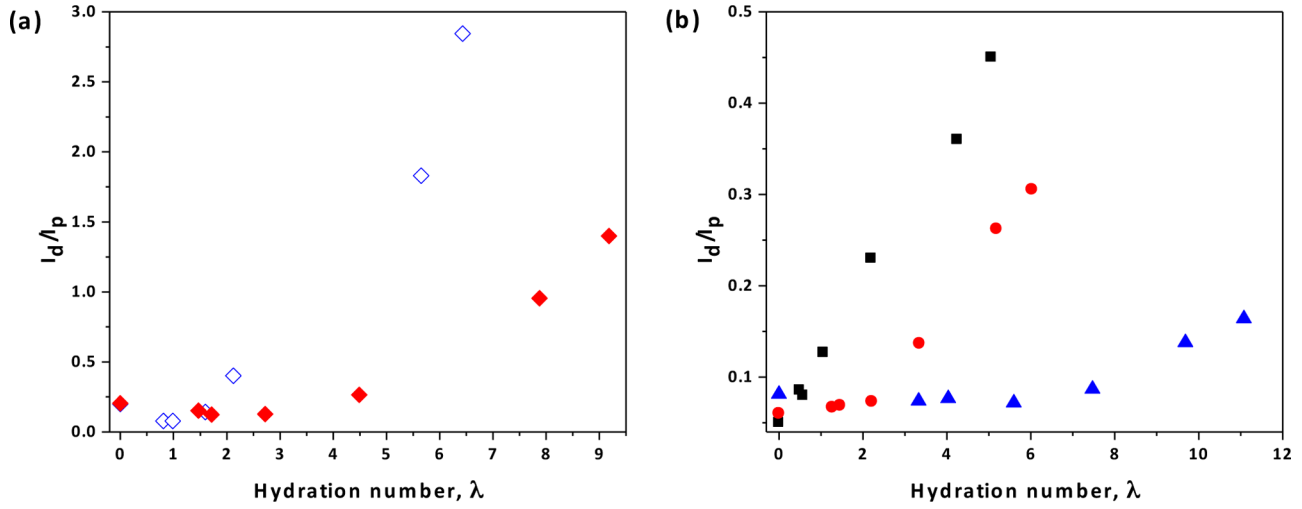

Figure 5. Ratio of fluorescence intensities of deprotonated to protonated state (I_d/I_p) of HPTS in (a) (red ◆) H^+- and (blue ◇) Na^+-form NAFION membranes and (b) H^+−NAFION thin films ((black ■) 590 nm, (red ●) 225 nm, (blue △) 70 nm) on n-SiO_2 as a function of hydration number (λ) .

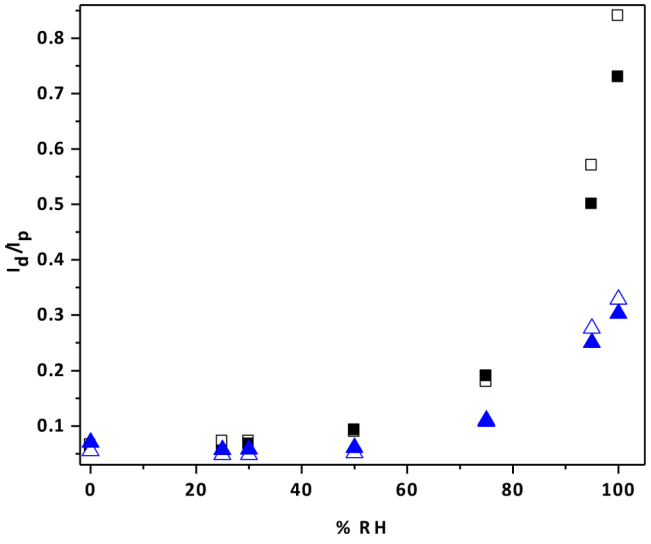

Figure 6. Ratio of fluorescence intensities of deprotonated to protonated state (I_d/I_p) of HPTS in H^+-form NAFION thin films on Au ((□) 588 nm, (blue △) 88 nm) and n-SiO_2 ((black ■) 590 nm, (blue ▲) 70 nm) surfaces as a function of water activity.

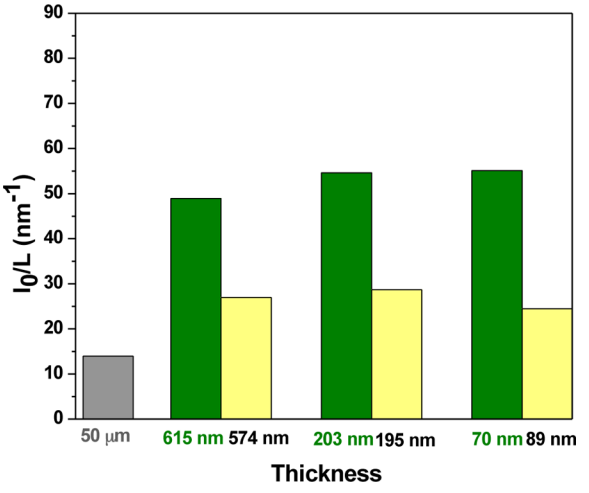

Figure 7. Normalized fluorescence intensity (I_0/L) of dry films on Au (yellow), n-SiO_2 (green), and membrane (gray) as a function of film thickness (L).

specific interactions, rather the decreasing domain size is simply a consequence of confinement of the film.

In addition to morphological effects where there may be isolated aqueous domains in thin polymer films, specific polymer−substrate interactions can suppress the dynamics of the polymer chains and thus stiffen the films and increase T_g.[33] The molecular mobility in thin films on n-SiO_2 and Au surfaces was investigated by calculating thickness-normalized fluorescence intensity (I_0/L) of CCVJ to estimate the rotational freedom of the dye incorporated into thin films and H^+-NR212 membrane in the dry state (Figure 7).

Gold has a broad absorption spectra with an adsorption maximum at around 520 nm.[52] Since the thin film samples were much thicker than the maximum energy transfer distance (<10 nm), the quenching effect induced by Au on CCVJ was negligible. The dye−polymer mass loading was maintained at 0.0018 wt % in polymer solutions to avoid dye concentration quenching and a small increase in I_0/L value was observed when the thickness of films on n-SiO_2 decreased from 615 nm (~49 nm^{-1}) to 70 nm (~55 nm^{-1}) films which indicates that the dry state stiffness of the thin films was slightly higher than for thick samples. A viscosity decrease or less restricted motion within the polymer sample lowered the fluorescence intensity of CCVJ and 50 μm thick membrane showed a lower value of I_0/L compared to the thin film samples. The thickness-normalized CCVJ fluorescence intensity showed that the polymer had higher mobility in thicker free-standing membranes compared to thin films which supports polymer−substrate interaction induced stiffening. Films on n-SiO_2 showed stronger dry state confinement (higher I_0/L) than films on Au at similar thicknesses which could be attributed to strong polymer−substrate specific interactions between NAFION and n-SiO_2.[49]

The local polymer and water mobility in thin films on two different substrates, n-SiO_2 and Au, were compared to free-standing membrane as a function of RH (Figure 8). I_0 and I_{RH} denote the fluorescence intensity of CCVJ in the dry state and at a given RH, respectively. In Figure 8a, the membrane became

dx.doi.org/10.1021/ma3011137 | *Macromolecules* 2013, 46, 413−421

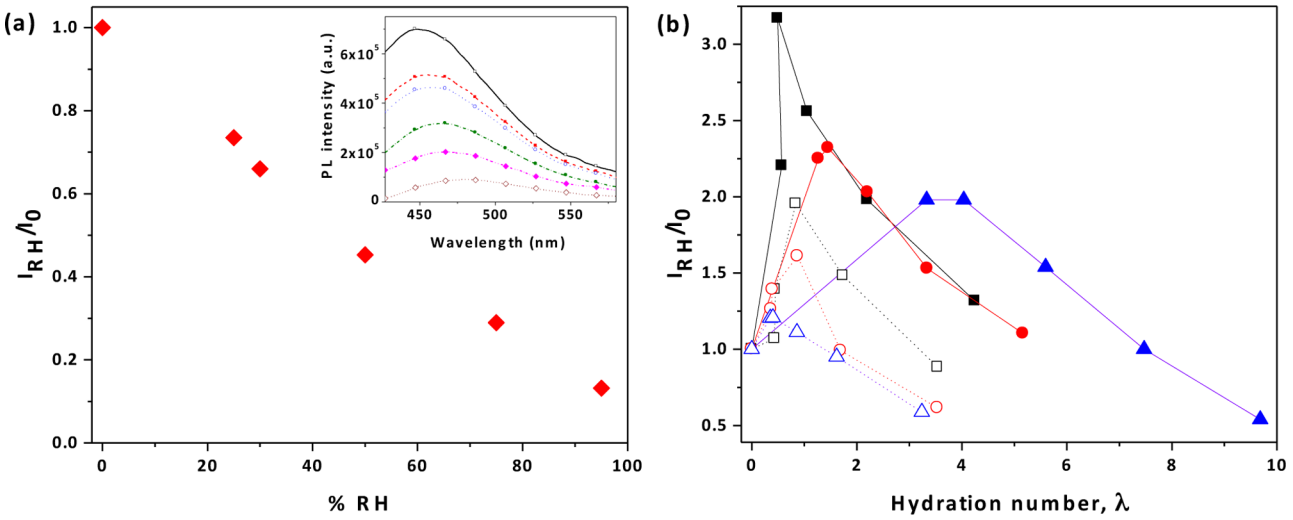

Figure 8. (a) Relative fluorescence intensity (I_{RH}/I_0) of CCVJ (λ_{exc} 400 nm) in H^+-NR212 membrane as a function of RH; inset shows the full spectra as a function of RH ((black □) 0%; (red ■) 25%; (blue ○) 30%; (green ●) 50%; (pink ◆) 75%; (brown ◇) 95%); (b) Effect of substrate on I_{RH}/I_0 in NAFION films with thicknesses (■) 615 nm (n-SiO_2), (black □) 574 nm (Au), (red ●) 203 nm (n-SiO_2), (red ○) 195 nm (Au), (blue ▲) 70 nm (n-SiO_2), and (blue △) 89 nm (Au) containing CCVJ as a function of hydration number, λ.

plasticized as the humidity was increased as reflected by a continuous decrease in the fluorescence of CCVJ. As opposed to membrane samples where the plasticization or a decrease in CCVJ intensity was observed, thin films showed an increase in fluorescence intensity at intermediate levels of RH, Figure 8b. The difference in antiplasticization behavior between samples on n-SiO_2 and Au stems from the stronger interactions of the acidic polymer with n-SiO_2. All thin films experienced increased hydration induced stiffening with increasing thickness at low-to-moderate relative humidity from 25% to 50%. Upon further hydration, the films began to plasticize.

Figure 9 shows the hydration number of thin films on n-SiO_2 and Au surfaces. Water uptake increased with decreasing thickness for films on n-SiO_2, while the hydration values of films on Au were lower and not sensitive to film thickness. The greater water uptake of films on n-SiO_2 could be attributed to the lamellar morphologies developed on this type of surface.[13] The extent of antiplasticization was significantly higher for thick films on n-SiO_2 compared to films on Au. In the case of 70 nm film on n-SiO_2, the dry state stiffness (Figure 7), antiplasticization (Figure 8b) and water uptake (Figure 9) were higher than the film with similar thickness (89 nm) on Au. This result suggests that for films on n-SiO_2, the sorbed water at the substrate interface enhances the interaction of polymer with substrate and actively takes part in the antiplasticization process, likely through hydrogen bonding between the polymer and the substrate.[53−55] The presence of water molecules adjacent to polar groups of NAFION in films on n-SiO_2 might initiate hydrogen bonding[54] between NAFION and SiO_2/-SiOH leading to greater film stiffening. On the contrary, the lack of affinity of water and the polymer for Au leads to higher mobility within the sample resulting in lower antiplasticization in films on Au.

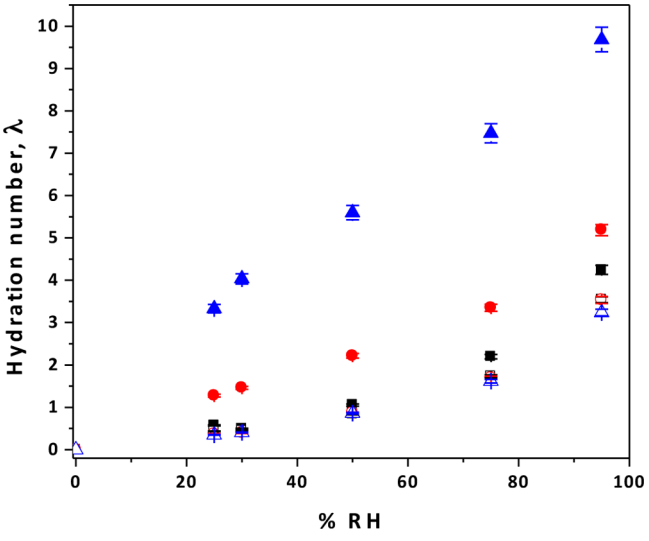

Figure 9. Hydration number (λ = n H_2O/n SO_3H) as a function of relative humidity (% RH) for films with different thicknesses on n-SiO_2 ((black ■) 615 nm; (red ●) 203 nm; (blue ▲) 70 nm) and Au ((□) 574 nm; (red ○) 197 nm; (blue △) 89 nm) surfaces.

Although the polymer confinement in dry films (I_0/L) was similar, RH-induced stiffening was impeded (low I_{RH}/I_0) in 70 nm films compared to thicker films on n-SiO_2 because of this sample's high water sorption. Figure 2 showed that deprotonation of HPTS was the lowest in the 70 nm film. The HPTS results point toward smaller hydrophilic domains in thin films and a water distribution with poor interchannel connectivity which was not able to support proton transport. However, distributed water may increase the plasticization of the sample and cause it not to stiffen as much with hydration. Thicker films showed greater antiplasticization and lower water uptakes, but better proton transport characteristics in HPTS experiments. These results support other observations where thicker films have greater proton conductivity than thin films.[4,56−58]

■ CONCLUSIONS

Measurements of two different fluorescent probes were adopted to track the local mobility and the proton solvation environment in thin NAFION films and membranes. NAFION films containing a photoacid probe (HPTS) revealed the importance of film thickness and its influence on the solvation environment within the sample. The solvation environment was

dx.doi.org/10.1021/ma3011137 | *Macromolecules* 2013, 46, 413−421

more favorable for proton transfer in 50 μm NR212 membrane compared to the solvation environment of thin films. As the film thickness was decreased, deprotonation of the dye (HPTS) decreased which indicated that the hydrophilic domain size in the films became smaller. This trend in small domain sizes with a decrease in film thickness was observed on both n-SiO_2 and Au substrates.

The local mobility of films and membranes were measured using a fluorescent rotor probe, CCVJ. Dry state polymer mobility (I_0/L) was the lowest for thin films on n-SiO_2, and thick/thin films on n-SiO_2 or Au had lower mobilities than membranes. Hydrated films on Au stiffened less with hydration due to the lower interfacial affinity between the polymer and the Au surface. Comparing the fluorescence properties of these two dyes to track proton dissociation and local mobility emphasizes the influence of interfacial confinement and specific polymer−substrate interactions on the properties of thin NAFION films.

■ ASSOCIATED CONTENT

Supporting Information

Additional figures showing fluorescence spectra and hydration number as a function of relative humidity.This material is available free of charge via the Internet at http://pubs.acs.org.

■ AUTHOR INFORMATION

Corresponding Author

*E-mail: hickner@matse.psu.edu. Telephone: 814-933-2204, Fax: 814-865-2917.

Notes

The authors declare no competing financial interest.

■ ACKNOWLEDGMENTS

The authors acknowledge the support of the US Department of Energy, the Office of Energy Efficiency and Renewable Energy, and the Fuel Cells Technology Program through a subcontract from General Motors Corporation under Grant DE-EE0000470.

■ REFERENCES

(1) Forrest, J. A.; Dalnoki-Veress, K. *Adv. Colloid Interface Sci.* **2001**, *94*, 167−196.
(2) O'Connell, P. A.; McKenna, G. B. *Science* **2005**, *307*, 1760−1763.
(3) Krtil, P.; Trojanek, A.; Samec, Z. *J. Phys. Chem. B* **2001**, *105*, 7979−7983.
(4) Paul, D. K.; Fraser, A.; Pearce, J.; Karan, K. *ECS Trans.* **2011**, *41*, 1393−1406.
(5) Park, S.-Y.; Jeong, H.; Kim, H.; Lee, J. Y.; Jang, D.-J. *J. Phys. Chem. C* **2011**, *115*, 24763−24770.
(6) Nagao, Y.; Iguchi, F.; Sata, N.; Yugami, H. *Solid State Ionics* **2010**, *181*, 206−209.
(7) Nagao, Y.; Ando, M.; Maekawa, H.; Chang, C. H.; Iguchi, F.; Sata, N. *ECS Trans.* **2009**, *16*, 401−406.
(8) Nagao, Y.; Naito, N.; Iguchi, F.; Sata, N.; Yugami, H. *Solid State Ionics* **2009**, *180*, 589−591.
(9) Tominaga, T.; Sano, K.-I.; Kikuchi, J.; Mitomo, H.; Ijiro, K.; Osada, Y. *Macro Lett.* **2012**, *1*, 2−6.
(10) Moilanen, D. E.; Fenn, E. E.; Wong, D.; Fayer, M. D. *J. Chem. Phys.* **2009**, *131*, 0147041−9.
(11) Mckenna, G. B. *Polymer Physics: From Suspensions to Nanocomposites and Beyond*; John Wiley & Sons, Inc.: New York, 2010; pp 191−223.
(12) Lin, E. K.; Kolb, R.; Satija, S. K.; Wu, W.-L. *Macromolecules* **1999**, *32*, 3753−3757.
(13) Dura, J. A.; Murthi, V. S.; Hartman, M.; Satija, S. K.; Majkrzak, C. F. *Macromolecules* **2009**, *42*, 4769−4774.
(14) Roth, C. B.; Dutcher, J. R. *J. Electroanal. Chem.* **2005**, *584*, 13−22.
(15) Frank, B.; Gast, A. P.; Russel, T. P.; Brown, H. R.; Hawker, C. *Macromolecules* **1996**, *29*, 6531−6534.
(16) Hall, D. B.; Torkelson, J. M. *Macromolecules* **1998**, *31*, 8817−8825.
(17) Miller, K. E.; Kruecer, R. H.; Torkelson, J. M. *J. Polym. Sci. B: Polym. Phys.* **1995**, *33*, 2343−2349.
(18) Priestley, R. D.; Ellison, C. J.; Broadbelt, L. J.; Torkelson, J. M. *Science* **2005**, *309*, 456−459.
(19) Levitt, J. A.; Chung, P.-H.; Kuimova, M. K.; Yahioglu, G.; Wang, Y.; Qu, J.; Suhling, K. *ChemPhysChem* **2011**, *12*, 662−672.
(20) Dishari, S. K.; Hickner, M. A. *Macro Lett.* **2012**, *1*, 291−295.
(21) Sone, Y.; Ekdunge, P.; Simonsson, D. *J. Electrochem. Soc.* **1996**, *143*, 1254−1259.
(22) Zawodzinski, T. A.; Neeman, M.; Sillerud, L. O.; Gottesfeld, S. *J. Phys. Chem.* **1991**, *95*, 6040−6044.
(23) Hietala, S.; Maunu, S. L.; Sundholm, F.; Lehtinen, T.; Sundholm, G. *J. Polym. Sci. B: Polym. Phys.* **1999**, *37*, 2893−2900.
(24) Eikerling, M. *J. Electrochem. Soc.* **2006**, *153*, E58−E70.
(25) Kreuer, K. D. *J. Membr. Sci.* **2001**, *185*, 29−39.
(26) Zawodzinski, T. A.; Springer, T. E.; Davey, J.; Jesterl, R.; Lopez, C.; Valerio, J.; Gottesfeld, S. *J. Electrochem. Soc.* **1993**, *140*, 1981−1985.
(27) Zawodzinski, T. A. *J. Electrochem. Soc.* **1993**, *140*, 1041−1047.
(28) Douhal, A.; Angulo, G.; Gil, M.; Organero, Ä.; Sanz, M.; Tormo, L. *J. Phys. Chem. B* **2007**, *111*, 5487−5493.
(29) Angulo, G.; Organero, J. A.; Carranza, M. A.; Douhal, A. *J. Phys. Chem. B* **2006**, *110*, 24231−242377.
(30) Moilanen, D. E.; Spry, D. B.; Fayer, M. D. *Langmuir* **2008**, *24*, 3690−3698.
(31) Spry, D. B.; Goun, A.; Glusac, K.; Moilanen, D. E.; Fayer, M. D. *J. Am. Chem. Soc.* **2007**, *129*, 8122−8130.
(32) Spry, D. B.; Fayer, M. D. *J. Phys. Chem. B* **2009**, *113*, 10210−10221.
(33) Keddie, J. L.; Jones, R. A. L.; Cory, R. A. *Faraday Discuss.* **1994**, *98*, 219−230.
(34) Fenn, E. E.; Wong, D. B.; Fayer, M. D. *Proc. Natl. Acad. Sci. U.S.A.* **2009**, *106*, 15243−15248.
(35) Bass, M.; Berman, A.; Singh, A.; Konovalov, O.; Freger, V. *Macromolecules* **2011**, *44*, 2893−2899.
(36) Wood, D. L.; Chlistunoff, J.; Majewski, J.; Borup, R. L. *J. Am. Chem. Soc.* **2009**, *131*, 18096−18104.
(37) Kongkanand, A. *J. Phys. Chem. C* **2011**, *115*, 11318−11325.
(38) Siroma, Z.; Kakitsubo, R.; Fujiwara, N.; Ioroi, T.; Yamazaki, S.; Yasuda, K. *J. Power Sources* **2009**, *189*, 994−998.
(39) Peron, J.; Mani, A.; Zhao, X.; Edwards, D.; Adachi, M.; Soboleva, T.; Shi, Z.; Xie, Z.; Navessin, T.; Holdcroft, S. *J. Membr. Sci.* **2010**, *356*, 44−51.
(40) Anpo, M.; Matsuura, T. *Photochemistry on Solid Surfaces*; Elsevier: New York, 1989.
(41) Lee, P. C.; Meisel, D. *J. Am. Chem. Soc.* **1980**, *102*, 5477−5481.
(42) Child, R. F.; Mika-Gibala, A. *J. Org. Chem.* **1982**, *47*, 4204−4207.
(43) Moilanen, D. E.; Spry, D. B.; Fayer, M. D. *Langmuir* **2008**, 143−150.
(44) Tielrooij, K. J.; Cox, M. J.; Bakker, H. J. *ChemPhysChem* **2009**, *10*, 245−251.
(45) Lakowicz, J. R. *Principles of Fluorescence Spectroscopy*; 3rd ed.; Springer: New York, 2010.
(46) Hauser, H.; Haering, G.; Pande, A.; Luisi, P. L. *J. Phys. Chem.* **1989**, *93*, 7869−7876.
(47) Zulauf, M.; Eicke, H.-F. *J. Phys. Chem.* **1979**, *83*, 480−486.
(48) Okada, T.; Møller-Holst, S.; Gorseth, O.; Kjelstrup, S. *J. Electroanal. Chem.* **1998**, *442*, 137−145.
(49) Ye, G.; Hayden, C. A.; Goward, G. R. *Macromolecules* **2007**, *40*, 1529−1537.
(50) Zeng, J.; Jean, D.-im; Ji, C.; Zou, S. *Langmuir* **2012**, *28*, 957−64.

(51) Fasolka, M. J.; Mayes, A. M. *Annu. Rev. Mater. Res.* **2001**, *31*, 323−355.
(52) Fan, C.; Wang, S.; Hong, J. W.; Bazan, G. C.; Plaxco, K. W.; Heeger, A. J. *Proc. Natl. Acad. Sci. U.S.A.* **2003**, *100*, 6297−6301.
(53) Seow, C. C.; Cheah, P. B.; Chang, Y. P. *J Food Sci* **1999**, *64*, 576−581.
(54) Gontard, N.; Guilbert, S.; Cuq, J.-L. *J. Food Sci.* **1993**, *58*, 206−211.
(55) Roussenova, M.; Murith, M.; Alam, A.; Ubbink, J. *Biomacromolecules* **2010**, *11*, 3237−47.
(56) Park, M. J.; Kim, S.; Minor, A. M.; Hexemer, A.; Balsara, N. P. *Adv. Mater.* **2009**, *21*, 203−208.
(57) Tylkowski, B.; Castelao, N.; Giamberini, M.; Garcia-Valls, R.; Reina, J. A.; Gumí, T. *Mater. Sci. Eng.: C* **2012**, *32*, 105−111.
(58) Lin, H.-L.; Yu, T. L.; Han, F.-H. *J. Polym. Res.* **2006**, *13*, 379−385.